SURFACE TOPOGRAPHY OF "HOTSPOT" REGIONS FROM A SINGLE CELL SRF CAVITY*

X. Zhao[#], G. Ciovati, C. E. Reece, and A. T. Wu
Jefferson Lab, Newport News, VA 23606, U.S.A.

Abstract

Performance of SRF cavities are limited by non-linear localized effects. The variation of local material characters between "hot" and "cold" spots is thus of intense interest. Such locations were identified in a BCP-etched large-grain single-cell cavity and removed for examination by high resolution electron microscopy (SEM), electron-back scattering diffraction microscopy (EBSD), optical microscopy, and 3D profilometry. Pits with clearly discernable crystal facets were observed in both "hotspot" and "coldspot" specimens. The pits were found in-grain, at bi-crystal boundaries, and on tri-crystal junctions. They are interpreted as etch pits induced by surface crystal defects (e.g. dislocations). All "coldspots" examined had qualitatively low density of etching pits or very shallow tri-crystal boundary junction. EBSD revealed the crystal structure surrounding the pits via crystal phase orientation mapping, while 3D profilometry gave information on the depth and size of the pits. In addition, a survey of the samples by energy dispersive X-ray analysis (EDX) did not show any significant contamination of the samples surface.

INTRODUCTION

There exists the frequent observation that SRF accelerator cavities made of high-purity bulk Nb (RRR~300) prepared using now customary chemical preparation techniques suffer "Q-drop" at field gradients above ~20 MV/m or ~100 mT. The causes of this phenomenon have not yet been fully elucidated. In addition, anomalous rf losses have been observed occasionally in the medium field range ($E_{acc} \cong$ 5-20 MV/m), causing a strong so-called "medium field Q-slope". Understanding the circumstances and mechanisms which cause enhanced RF losses in this medium field range is important for the development of CW superconducting accelerators. To contribute to the study of this topic, a surface analysis study was undertaken on samples cut from a single cell cavity made of large-grain Nb which exhibited a strong medium field Q-slope, therefore offering the opportunity to investigate among the possible sources of enhanced RF losses. Samples were cut from locations where anomalous heating was detected by thermometry ("hotspots") as well as from locations with negligible overheating ("coldspots").

PREPARATION OF SAMPLES

The investigated single cell 1.5 MHz SRF cavity is made of a large grain plate cut from ingot B produced by Companhia Brasileira de Metalurgia e Mineração (CBMM, Sao Paulo, Brasil). Ingot B had several large grains in-plane. RRR value of the material was ~280 with a Ta content of ~800 ppm. Results on other single cells built from this material are shown in [1]. The cavity had experienced the following processes:

- Large grain sheets sliced from ingot "B" (CBMM) by wire-EDM
- A deep-drawing process deforming the plates to half cells
- Prior to the equator weld, ~ 10 min etching by Buffered Chemical Polishing (BCP) with HNO_3, HF, H_3PO_4 1:1:1 by volume
- Electron beam weld was done inside and outside.
- After welding, the weld was mechanically ground
- The beam tubes were welded in the end to the irises
- The cavity was heat treated at 600°C/10h, then etched ~ 10+60 µm by BCP 1:1:1 before first rf test

Buffered chemical polishing (BCP) is a standard process to treat SRF cavity and is a necessary step in order to remove a damage layer introduced by EDM cutting, die deforming, mechanical grinding. During polishing, phosphoric acid acts as a buffer, and nitric acid is an oxidizing agent toward which produces niobium pentoxide (Nb_2O_5). Hydrofluoric acid reacts with Nb_2O_5 and produces soluble Nb-fluoride or Nb-oxifluoride.

The results of the first rf test at 1.7 K are shown in Figure 1. The quality factor, Q_0, monotonically decreased for increasing peak surface magnetic field, B_p, up to 68 mT, where quench occurs. The cavity performance did not improve significantly after an additional 30 µm etching by BCP 1:1:1. Temperature mapping showed the quench location to be on the cell's side wall, closer to the iris. A large defect ("hole") was visible by naked eye in that area. Repair of the defect was attempted by mechanical grinding, followed by an additional ~70 µm removal by BCP 1:1:1. The following rf test showed an improvement of the quench field, occurring at the same location as before. The Q_0 vs. B_p curve was still characterized by a strong medium field Q-slope. No field emission was detected during any of the RF tests. Figure 2 shows an "unfolded" temperature map just below the quench during test No. 3. Several "hotspot" are visible in the equator area. The location of the hotspots did not change significantly with successive material removal by BCP.
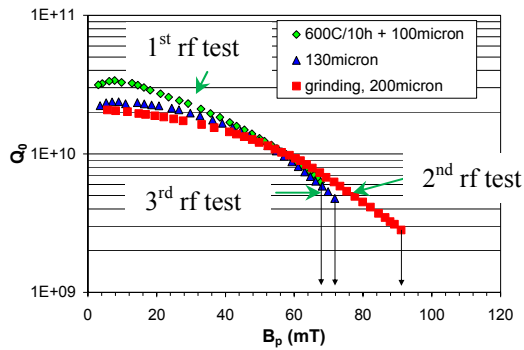
Figure 1: Q_0 vs. B_p at 1.7 K after successive material removal showing a strong medium field Q-slope.
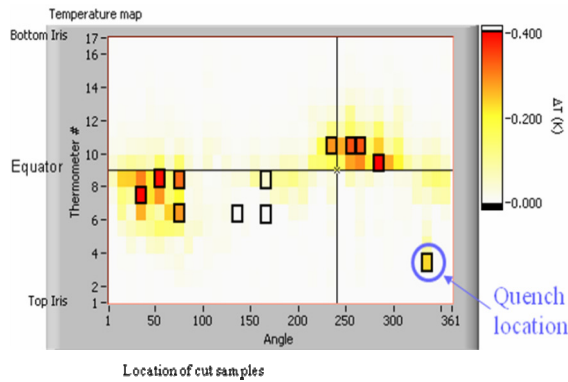

Figure 2: Twelve samples (nine from "hotspots" and three from "coldspots") were cut from the cavity by milling for surface analysis.

ANALYSIS OF SAMPLES

Twelve 12 mm × 12 mm samples were cut from locations on the cavity shown in Figure 2 by careful milling, using water as coolant. For comparison, three coupons were from normal areas (called coldspots zone), eight from hotspots zones and one included the quench location. Optical and scanning electron microscopes were used to observe the samples surface. Other than mechanical scratches attributed to the cutting process, the most obvious features are "pits" along bi-crystal grain boundary, tri-crystal junction, and sometimes in the middle of an ultra flat crystal grain plane. The pits share similar features: they have clear facets. Features of these samples are briefly described in Table 1. It is known that such pits can be induced by chemical etching processes [4-5], therefore we refer to the abnormal pitting features as "etching-pits." BCP etching left very sharp boundaries along crystal grain, as observed by either optical microscopy or SEM. It was qualitatively observed that the coldspot samples had a lower pit density than some of the hotspot samples. Particularly, only one etching-pit was observed on sample No. 8. Sample No. 9 (Figure 3) has more than 1000 pits and the pit-density on one grain is very much higher than on the other. The typical size of the pits, measured with a 3D profilometer, ranges between 20-80 μm in width and 2-10 μm in depth.

Table 1: Features Observed on Samples Dissected from the Large-Grain Single Cell Cavity.

Sample No.	No. of grains	Location	Etch-pits feature
1	1	Hotspot	
2	2	Quench site	High density
3	3	Hotspot	
4	2	Hotspot	
5	3	Hotspot	High density; a very deep pit on tri-crystal junction
6	1	Coldspot	Low density
7	3	Coldspot	A shallow pit on tri-crystal junction
8	1	Coldspot	Only one pit found
9	3	Hotspot	High density; a very deep pit on tri-crystal junction
10	1	Hotspot	
11	2	Hotspot	High density
12	2	Hotspot	High density

Samples No. 3, 5, 7, 9 each consist of three large crystal grains. Etching pits are found at all the tri-crystal junctions. (See Figures 4-6.) At the junction, the profile of the etching pit of sample No. 7 is much shallower than the others. Other etching pits at the tri-crystal junctions are deep, sharp and have many facets. Etching pits were also observed within crystal grains (Figure 7). The etching pits were thus clearly not just restricted to grain boundaries.
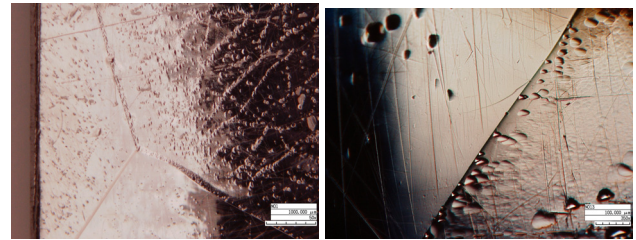

Figure 3: Optical microscopy images of sample No. 9, showing high density of etching pits (left) and non-uniform; pit distribution (right).
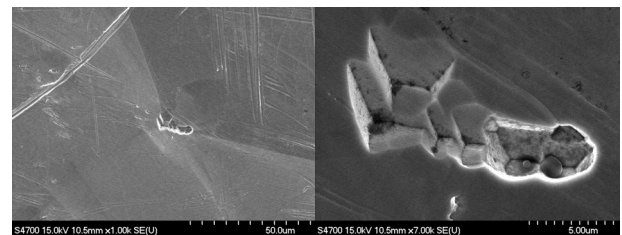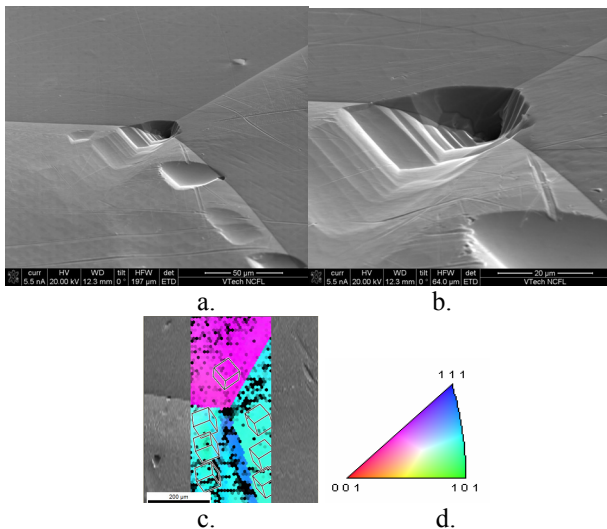

Figure 4: Etching pit of sample #7.

Figure 5: a-b) Etching pit at tri-crystal junction (sample #9); c) Crystal orientation map via EBSD revealing the three crystal orientations; d) EBSD color map legend.
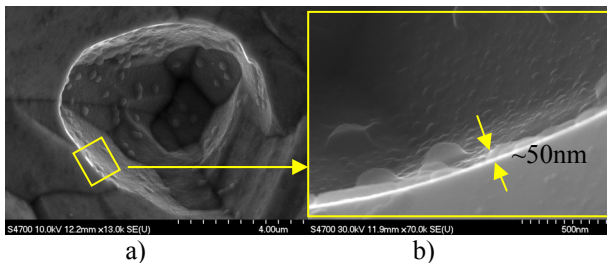

Figure 6: a-b) from sample#5. Etching pits at tri-crystal junctions have deep, sharp profiles. The pit diameter is ~5 μm and its curvature radius ~50 nm. Thus its aspect ratio is ~100.
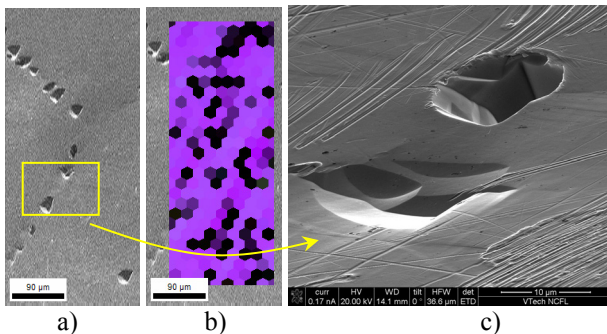

Figure 7: Etching pits on a single crystal grain. Photos were taken on sample #3. a) a SEM micrograph; b) inverse pole figure (IPF) surveyed by EBSD indicating a single crystal zone.

The pits shown in Figure 7a may be distributed along a dislocation slip path within the single grain. Cai [4] reported that the etching pits' profile directly correlates with the orientation of the exposed crystal surface. Since various crystal planes have different surface energy, they yield difference etching rate. Anisotropic etching rates thus yield the symmetric and facet features of the pits.

EDX analysis performed on all samples did not show any significant contamination of the Nb surface. The areas surrounding and inside a pit have been analyzed by Auger electron spectroscopy, also indicating no impurities.

DISCUSSION AND SUMMARY

The analysis of the surface topography of samples cut from a large-grain single cell characterized by a strong medium field Q-slope revealed a high density of etching pits. These were found to be distributed both along grain boundaries and within grains, the latter case possibly being related to the presence of lattice defect, such as dislocations, or impurities. Etching pits observed in this study are uncommon to the surface of large-grain BCP-etched cavities, and the cause for their nucleation on this particular cavity is still unclear.

Although it has been shown, both by experiments [6] and simulations [2], that magnetic field enhancement at sharp edges, such as grain boundaries, pits or other defects, may cause local and/or global quench, RF and temperature measurements of this cavity indicate monotonic losses, already starting at very low field (B_p ~ 20 mT). The hypothesis of local intermediate state transitions, such as suggested by Knobloch et al. [7], starting at such low field would imply a field enhancement factor of about 10. Pits 50 μm in diameter would require radii of curvature of order 50 nm to produce this field enhancement [2]. Although corners this sharp are present in the pit of Figure 6, features with the aspect ratio of ~1000 have not yet been observed.

ACKNOWLEDGMENTS

REFERENCES

[1] P. Kneisel, G.R. Myneni, G. Ciovati, J. Sekutowicz, T. Carneiro, "Development of Large Grain/Single Crystal Niobium Cavity Technology at Jefferosn Lab", Single Crystal Niobium Technology Workshop, CBMM, Araxa, Brazil, Nov. 2006.

[2] V. Shemelin, H. Padamsee, TTC-Report 2008-07, SRF 080903-04, TESLA 2008.

[3] H. Padamsee, S0 Meeting, Jan 26, 2009.

[4] B.C. Cai, A. Dasgupta and Y.T. Chou, Journal of the Less-Common Metals, 90(1983) 37-47.

[5] P.R.V. Evans, Journal of the Less-Common Metals, 6(1964) 253-265.

[6] S. Berry, C. Antoine and M. Desmons, "Surface Morphology at the Quench Site", EPAC'04, Lucerne, July 2004, TUPKF018, p. 1000 (2004).

[7] J. Knobloch, R.L.Geng, M. Liepe, and H. Padamsee, "High-Field Q Slope in Superconducting Cavities Due to Magnetic Field Enhancement at Grain Boundaries," 1999 SRF Workshop, Santa Fe, TUA004.